Appl Phys A
DOI 10.1007/s00339-010-5819-5

Applied Physics A
Materials Science & Processing

Direct writing of micro/nano-scale patterns by means of particle lens arrays scanned by a focused diode pumped Nd:YVO_4 laser

Ana Pena · Zengbo Wang · David Whitehead · Lin Li

Received: 13 November 2009 / Accepted: 10 May 2010
© Springer-Verlag 2010

Abstract A practical approach to a well-known technique of laser micro/nano-patterning by optical near fields is presented. It is based on surface patterning by scanning a Gaussian laser beam through a self-assembled monolayer of silica micro-spheres on a single-crystalline silicon (Si) substrate. So far, the outcome of this kind of near-field patterning has been related to the simultaneous, parallel surface-structuring of large areas either by top hat or Gaussian laser intensity distributions. We attempt to explore the possibility of using the same technique in order to produce single, direct writing of features. This could be of advantage for applications in which only some areas need to be patterned (i.e. local area selective patterning) or single lines are required (e.g. a particular micro/nano-fluidic channel). A diode pumped Nd:YVO_4 laser system (wavelength of 532 nm, pulse duration of 8 ns, repetition rate of 30 kHz) with a computer-controlled 3 axis galvanometer beam scanner was employed to write user-defined patterns through the particle lens array on the Si substrate. After laser irradiation, the obtained patterns which are in the micro-scale were composed of sub-micro/micro-holes or bumps. The micro-pattern resolution depends on the dimension of both the micro-sphere's diameter and the beam's spot size. The developed technique could potentially be employed to fabricate photonic crystal structures mimicking nature's butterfly wings and anti-reflective "moth eye" arrays for photovoltaic cells.

A. Pena (✉) · Z. Wang · D. Whitehead · L. Li
Laser Processing Research Centre, School of Mechanical, Aerospace and Civil Engineering, The University of Manchester, Manchester, M60 1QD, UK
e-mail: Ana.Pena@postgrad.manchester.ac.uk

1 Introduction

In recent years an increased interest in replicating natural behaviours (also known as biomimetism) has attracted a lot of research effort [1, 2]. Research on the micro-nano-structure of butterfly wings has shown them as natural photonic crystals. This has established a strong link between the vivid wing colours and the morphology of the wings [3]. Insects use light manipulation as a means to signal between one another but also for thermoregulation and camouflage purposes. The object of such recent interest on natural photonic structures has its roots in the engineered design by which living organisms manipulate and control light to fulfil specific needs [4]. Structure periodicity dictates the way light behaves when encountering a surface (i.e. reflection, absorption and transmission). To be able to control light in the optical spectrum, structuring of materials has to be done within the same scale typically ranging from hundred nanometres to several micrometres. Dimensions of periodicity (1D, 2D or 3D) affect the electromagnetic band gap of the material in the visual wavelength range [5], which could change surface colour or form anti-reflective surfaces. These surfaces are known as "moth eye", "nipple arrays" or "subwavelength structures (SWS)" [6–11]. In nature they appear in the eyes of some insects helping them to enhance the photon collection of their visual system and to reduce reflection that could attract predators.

Vukusic found recently that nano-structures on the wing scales of some butterflies enhance optical absorption by 90 to 95% resulting in enhanced black colouration [12]. The explanation for such an effect is attributed to the effective medium theory which states that a subtle change in the optical impedance between two mediums will reduce Fresnel reflection. Many micro- and nano-fabrication techniques could fulfil the challenge of fabricating photonic structures

Published online: 17 June 2010

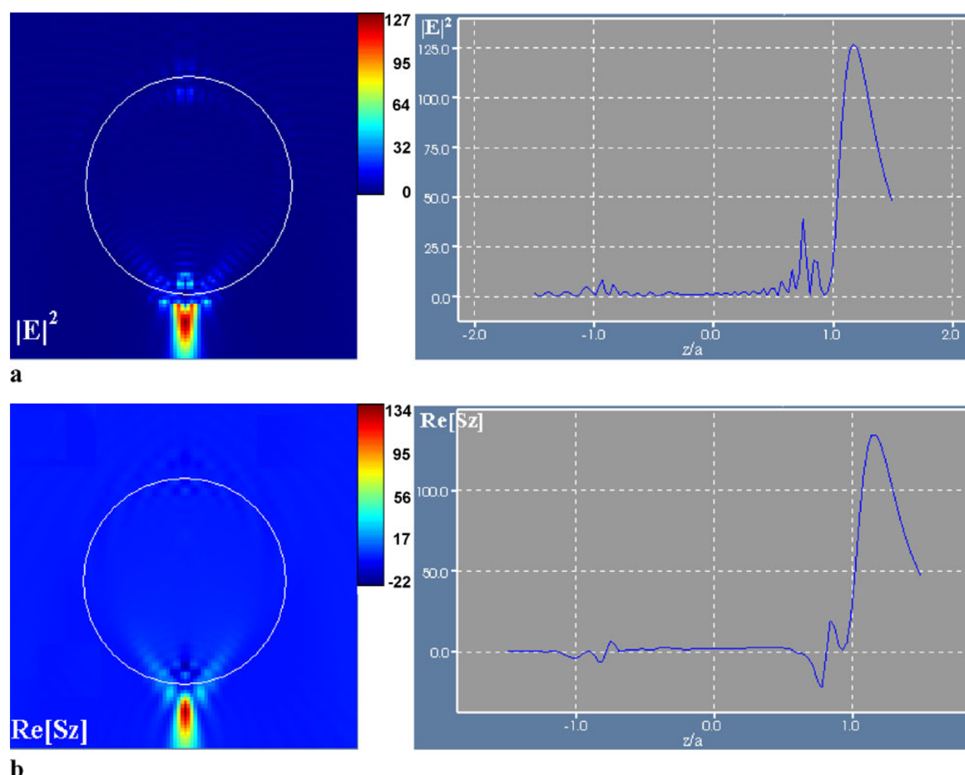

Fig. 1 Cross sectional view of the normalised local field distribution: (**a**) $|E|^2$; (**b**) $\mathrm{Re}[S_z]$ underneath a 5 μm SiO_2 micro-sphere in air (incident laser beam of wavelength $\lambda = 532$ nm, pulse duration of $\tau = 8$ ns)

in a diversity of materials [13–24]. In the long term, only the most economic and feasible ones will prevail as the accepted method of fabrication. We attempt to demonstrate how a widely-recognised near-field nano-patterning technique could be used to fabricate custom-defined single-line micro/nano-structures, or to create 2D photonic structures in delimited areas exhibiting distinct shapes (i.e. curves, lines, spiral forms, letters) instead of simultaneously patterning millions of features over large areas as it has been done until now. This novel approach is presented in this paper based on a technique termed by other authors as a "Contact Particle-Lens Array" technique which relies on the near-field enhancement effect by small particles interacting with a laser beam.

2 Theory

In the Contact Particle-Lens Array (CPLA) technique, the particle mask consists of a self-assembled monolayer which offers massive, parallel nano-structuring with a significant improvement in patterning speed under single laser pulse radiation [25–29]. This near-field patterning mechanism was first identified after surface damage appeared during the process of particle removal by dry laser cleaning (DLC) [30, 31]. The technique was further developed by many authors who have studied the near-field effects of small particles on a substrate when subjected to laser irradiation [32–37]. Transparent spherical particles which compose the monolayer are used as a lens array for focussing far-field laser radiation. The near-field lens array produces a strong field enhancement at each particle-sample contact point. Due to the involvement of evanescent waves, the near-field foci can be scaled below the diffraction limit [25, 38] i.e. super-resolution effect. In order to show the basic physics of the near-field focussing effect induced by a small particle, Mie's theory modelling of the optical near field around a single particle was carried out. Figure 1 shows the modelling results in a cross sectional view of the normalised local intensity field distribution (normalised electric field intensity $|E|^2$ and the real part of the z-component of normalised Pointing vector $\mathrm{Re}[S_z]$) underneath a particle (diameter of 4.74 μm, refractive index of 1.45) in air, when subjected to an x-polarised plane wave excitation at a wavelength of 532 nm, and pulse duration of 8 ns. By comparing Fig. 1(a) and Fig. 1(b), one can clearly see that the field distribution of $|E|^2$ differs from the $\mathrm{Re}[S_z]$ field distribution. The difference, again, arises due to the presence of the evanescent wave components in the near-field regions. From Fig. 2(a) and (b), it can also be seen that the focus point for such a particle (in air) is at a position $z/a = 1.2$; very close to the particle surface. It can also be seen that the near-field enhancement decays to half its maximum in the range from $z/a = 1.2$ to $z/a \sim 1.455$ which means that a sample must be kept in near-field distance with the particle lens array for

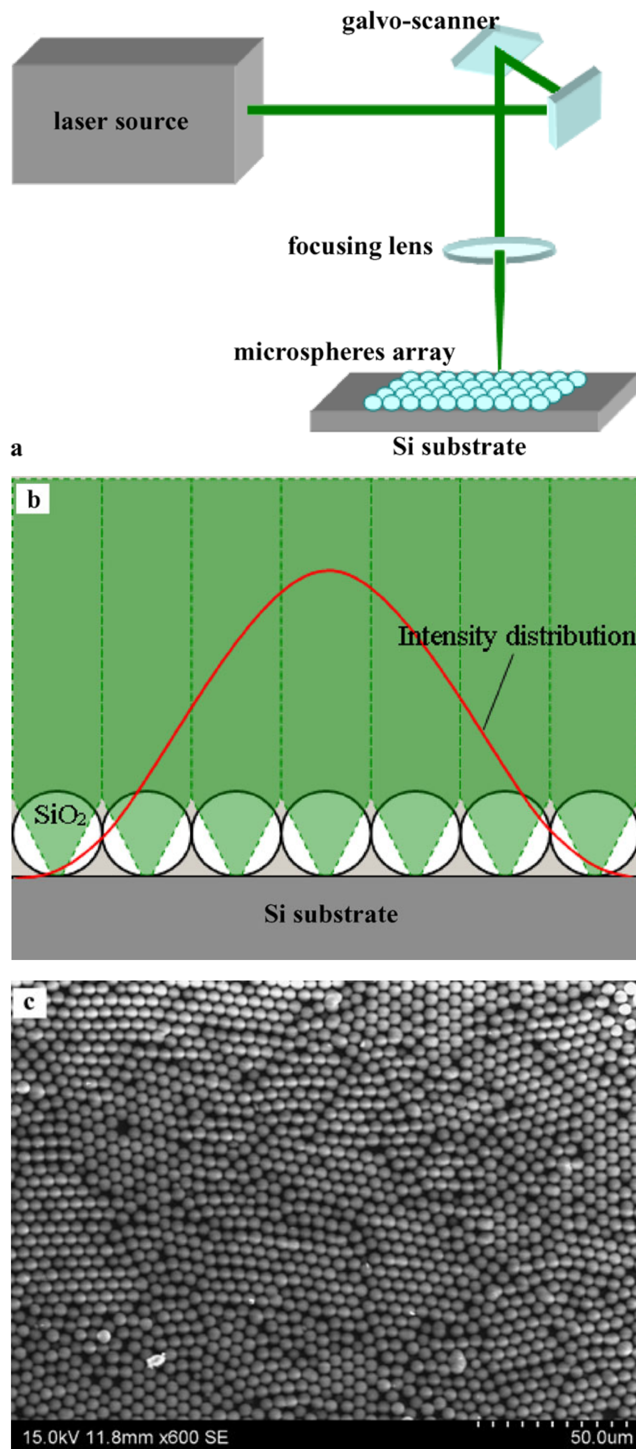

Fig. 2 Schematic views of: (**a**) experimental setup; (**b**) focused laser beam scanned over the SiO_2 monolayer (to scale: 5 μm diameter SiO_2 micro-sphere); (**c**) scanning electron micrograph (SEM) of a self-arranged monolayer formation of 5 μm SiO_2 micro-spheres

efficient patterning. It should be noted that the current simulation is limited to the simplest case of a single particle subjected to laser irradiation based on classical Mie theory. To include influences of substrates and neighbouring particles on the focussing and near-field distributions, numerical modelling techniques have to be used. This approach along with detailed information on optical near fields in different particle-substrate systems (particle aggregates, particle on substrate, particle in solution, etc.) has been reviewed in one of our recent papers [39].

3 Experimental

The experimental setup is portrayed in Fig. 2(a). The used sample is a p-type single-crystalline Si wafer, <100> orientation, boron doped with resistivity of 1–10 Ω cm. A diode pumped Nd:YVO_4 laser system (Laserval Violino, wavelength of $\lambda = 532$ nm, pulse duration of $\tau = 8$ ns, and a repetition rate of 30 kHz) was applied as the light source. A computer-controlled three-axis Galvanometer beam scanning system is attached to the laser system, allowing fabrication of arbitrary patterns on the sample surface.

In the experiments, the samples were first cleaned with acetone and methanol, followed by a de-ionised (DI) water rinse and then dried. A drop coating method was then utilised to deposit a uniform monolayer of silica (SiO_2) micro-spheres onto the sample surfaces. After this a hexagonal array of particles was formed by a self-assembly process where the quality of the monolayer depends on many factors such as the cleanliness of the surface, wettability, temperature and any environmental disturbance. The obtained monolayer mask in our experiments is shown in Fig. 2(c), and was in reasonably good quality over a large surface area. The non-porous SiO_2 micro-spheres (refractive index of ∼1.43–1.46, mean diameter of 4.74 μm) utilised in our experiments were initially buffered in DI water with a 9.8 (wt%) solids content.

The prepared samples coated with particles were then processed with a Gaussian laser beam. The laser focus is in an elliptical shape with a spot size of ∼50 μm along minor axis and ∼80 μm along major axis. The applied laser fluences were set below the ablation threshold of bare Si in the reported experiments. At laser fluences below ∼200 mJ/cm^2, no apparent material modification takes place on a bare surface. However, due to the field enhancement effect given by the particles, ablation took place at the sites where micro-spheres were located, see Fig. 4. In this way, arbitrary patterns of width in the same scale as the beam size are composed of sub-micrometre structures due to the combination of the conventional laser direct micro-fabrication technique and the CPLA technique. To the best of our knowledge, such a kind of double-scale texturing (i.e. micro-sized patterns made of sub-micron and/or nano-structures) is reported for the first time. Though in the past several authors have detailed the use of focused Gaussian beams in order to produce nano-patterns in a variety of substrates [40–42], it has not been proposed yet how a focused

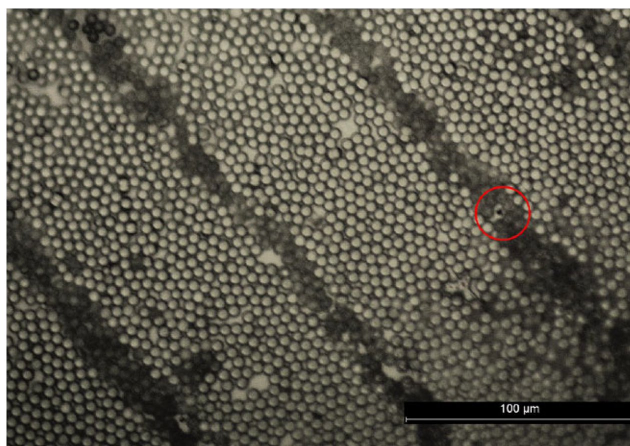

Fig. 3 Optical micrograph of a micro-spheres monolayer after laser irradiation by a focused Gaussian beam. SiO_2 micro-spheres remained in the surface on top of the generated sub-micro/micro-structures which explains the change in reflectivity. Also shown is the site were a micro-sphere was removed leaving a hole behind (shown inside the circle)

beam can be scanned across a monolayer formation in order to obtain single patterns instead of massive, parallel structuring.

In the experiments the pulse repetition rate was set as 30 kHz and the scanning velocities were varied from 1000 to 5 mm/s, which resulted in multiple pulses being delivered to each spot for the lowest velocities. Although most of the particles can be removed after a single-pulse irradiation, it was noticed that for the lowest fluence applied (150 mJ/cm^2) some particles remained on top of the sub-micro-structures possibly due to a small tilt in the scanning beam path. This can be seen in Fig. 3 in which a variation in reflectivity is present in the locations where the Gaussian beam was scanned. The rest of the particles that remained in the areas where the laser beam was not scanned, were removed after the process by sweeping a lens cleaning tissue over the surface. The processed samples were characterised by employing an Optical Microscope (OM, Polyvar MET), a Scanning Electron Microscope (SEM, Hitachi S-3400N) and Atomic Force Microscopy (AFM, Veeco Innova Scanning Probe Microscope).

The patterns shown in Fig. 4(a–c) were generated by the above described technique at laser fluences of 150–200 mJ/cm^2, scanning velocity of 5 mm/s and laser repetition rate of 30 kHz (this implies a delivery of 300 pulses per spot). The contrast between the laser scanned lines and the bare substrate is given by the scattering effects of the different generated sub-micro/micro-metre structures. The width of the laser-scribed lines at a fluence of 200 mJ/cm^2 is ∼72 µm and descends to 34 µm at a fluence of 150 mJ/cm^2. Further reductions in width are observed in Fig. 4(d) if the scanning velocity is increased to 100 mm/s (15 pulses per spot) which results in a 24 µm line (formed by about 5 sub-

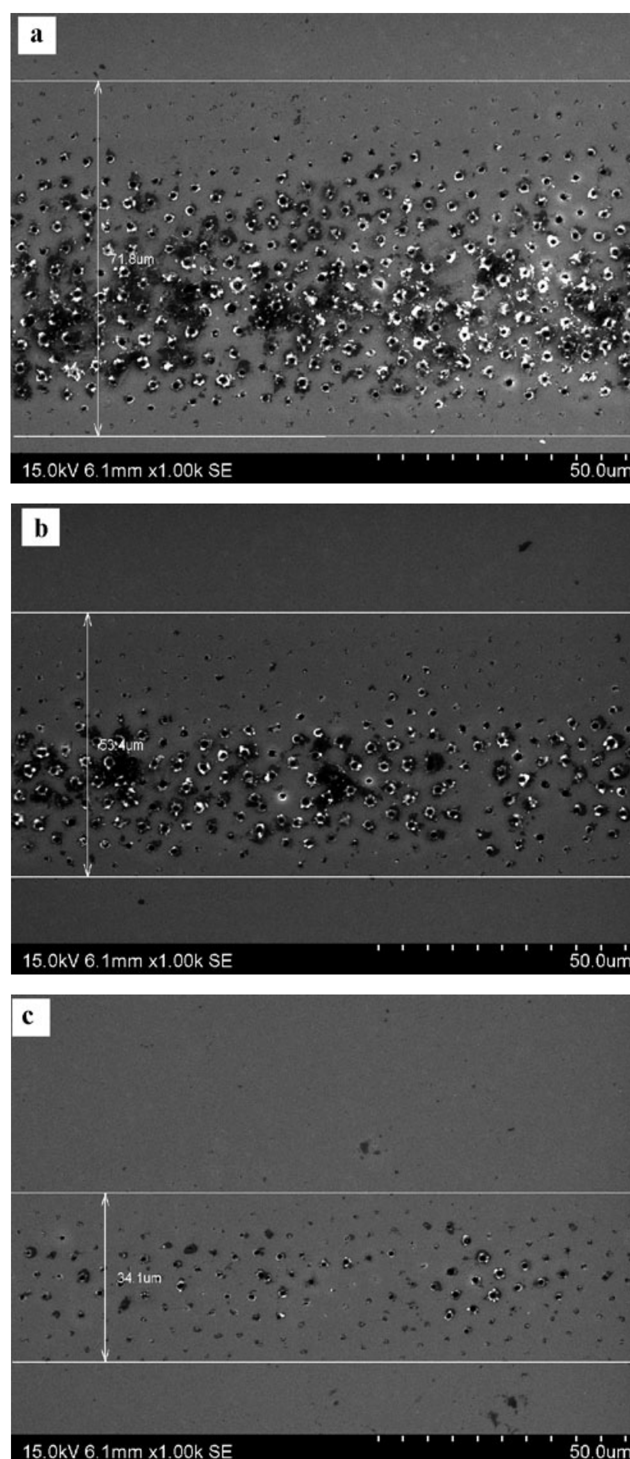

Fig. 4 SEM images of micro-scale lines made of sub-micrometre structures generated after a focused beam was scanned over a 5 µm spheres array: (**a**) fluence of 200 mJ/cm^2, scanning velocity of 5 mm/s, line width of 72 µm; (**b**) fluence of 170 mJ/cm^2, line width of 53 µm; (**c**) fluence of 150 mJ/cm^2, line width of 34 µm; (**d**) fluence of 150 mJ/cm^2, scanning velocity of 100 mm/s, line width of 24 µm; (**e**) fluence of 150 mJ/cm^2, a scanning velocity of 1000 mm/s (1 m/s) results in the individual mark for each pulse per spot; (**f**) fluence of 150 mJ/cm^2 might also generate amorphisation of Si in the periphery of the elliptical beam

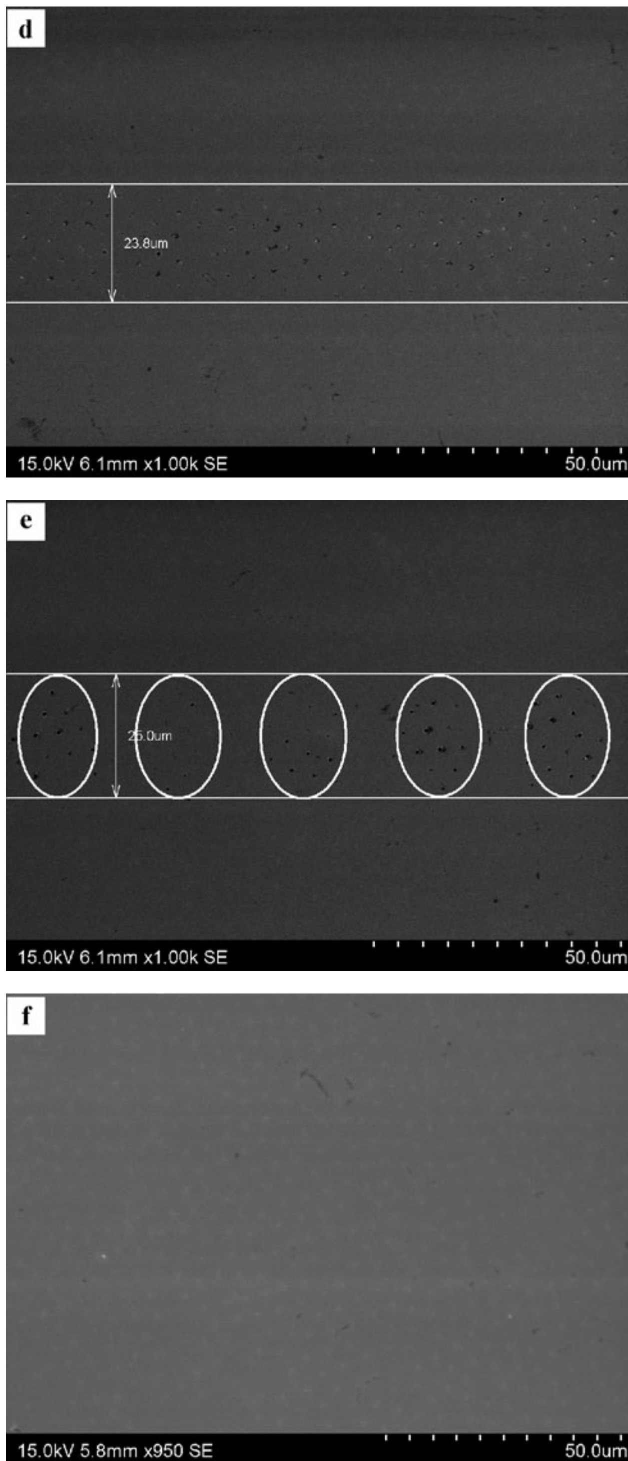

Fig. 4 (*Continued*)

micro-structures across the minor axis of the beam), this is smaller than the laser spot size of 50 μm × 80 μm. Due to limitations of our current system it has not been possible to decrease the far-field focal spot size so only a single line of particles is irradiated, but work is being undertaken in order to further reduce such a parameter. Shown in Fig. 4(e) is the effect of depositing only one pulse per spot in the monolayer formation, where the elliptical shape of the beam is clearly appreciated.

4 Discussion

The decrease in sub-micro-structure size in the lateral edges of the laser-scribed lines seen in all the SEM images of Fig. 4 occurred due to very low fluences beneath the peripheral micro-spheres irradiated by the Gaussian beam. Such low fluence values also resulted in the amorphisation of Si under the micro-spheres at these particular edges. The characteristic "white" halo structures seen in amorphised Si [43–45] are presented in Fig. 4(f).

The AFM image in Fig. 5(a) clearly shows the different surface morphologies of ablated sub-micro-structures by a focused Gaussian beam. A change in the height profile according to the laser distribution is clearly defined from the outer part towards the central part of the beam, where structures are at their highest because of the accumulation of molten material in the form of a bump reaching ∼250 nm in height. On the contrary, structures formed at the edges of the Gaussian distribution manifest bumps of height ∼10 nm height and craters of depth ∼10 nm.

A more accurate profile dimensional analysis was done for different morphologies and their different profiles are shown in Fig. 5(b–d), where it can be observed that craters, bumps and "sombrero" shapes can be found across the major axis of the elliptical spot. The larger structures (craters with significant debris around them and bumps formed by debris accumulation) were formed when the central part of the beam was scanned over the contact particle lens array. Their formation is clearly related to the near-field enhancement given by the contact particle lens array when irradiated by the laser beam. Considering the laser intensity near-field enhancement under the micro-spheres and the employed nanosecond laser, photo-thermal ablation in the form melt-expulsion/redistribution could be acknowledged as the material removal mechanism in this process [46–48]. Smaller bumps like the one shown in Fig. 6 can be found in the periphery of the ablation spot, the formation mechanism in this case is different and can be explained by a lower intensity enhancement that can cause convective fluxes inside the melt pool due to surface tension (thermo-capillary effect) [49].

Different computer designed patterns could be easily transferred to the samples by utilising the integrated galvo-scanning system. The obtained results are shown in Fig. 7(a–d), where a high contrast in the images is given by the scattering effects of the laser-generated sub-micro/micro-metre structures described above. This pattern-

Fig. 5 (**a**) Atomic force microscopy image of a micro-scale line formed by sub-micrometre structures and the respective height profile across the width of the line, which shows a variation in structure height according to the laser intensity distribution; (**b–d**) Different height profiles of some of the structures found along the beam's intensity distribution

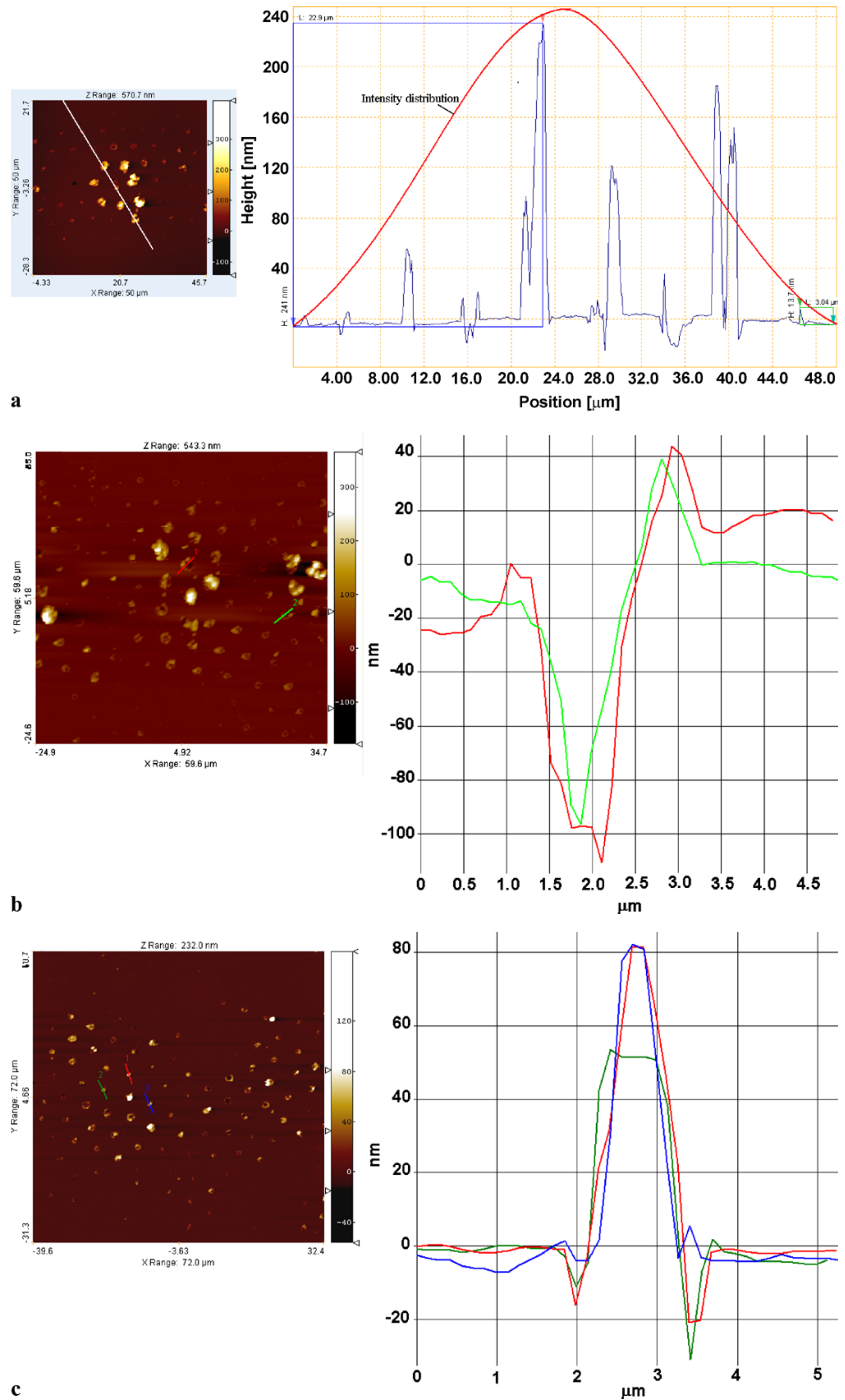

Fig. 5 (*Continued*)

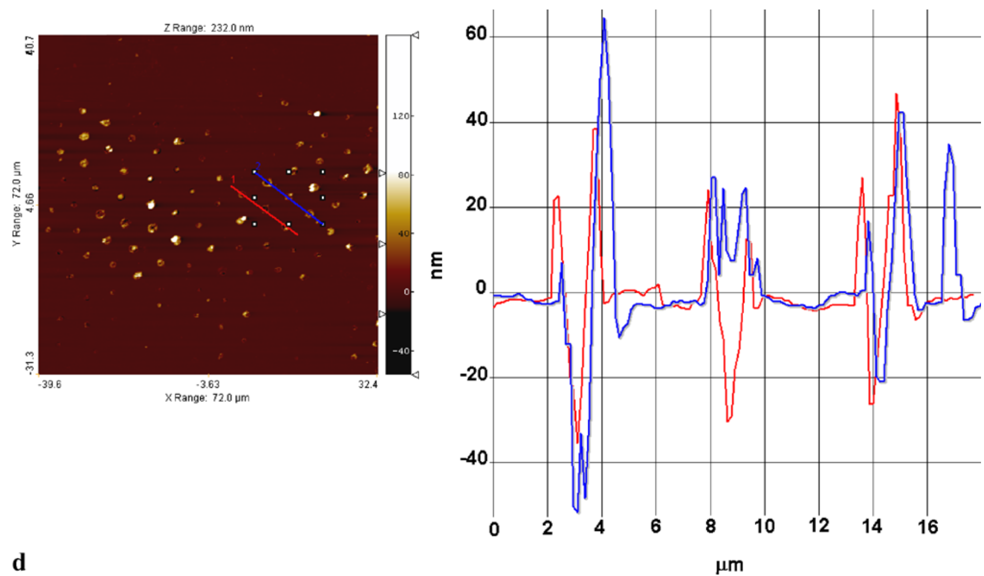

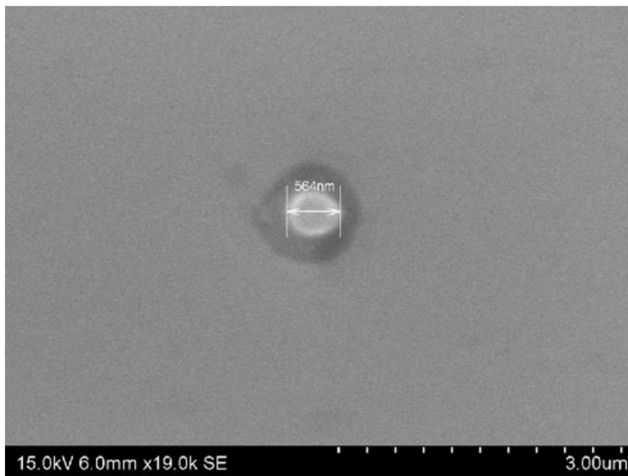

Fig. 6 SEM image of a Si nano-bump found in the periphery of the ablation spot size

ing technique is intended to be further developed in order to decrease the line lateral dimension by employing a tighter spot size and smaller micro-sphere diameters. In Fig. 8, the ideal scanning path of a focused beam over a pre-defined pattern is portrayed and it could be made possible if the spot size is further reduced so only a single micro-sphere is irradiated by one pulse at a time. This could lead to the production of lines or features made of nano-structures assuming that the correct parameters are selected (i.e. fluence value, micro-sphere size). Moreover, by consecutively changing the angle at which the beam reaches the micro-spheres array and by delivering several pulses at the same location, continuous lines with a lateral dimension below the diffraction limit could be generated by connecting several ablation sites under the same micro-sphere. So far this technique of using an angular laser scanning beam over a self-assembled monolayer has been used to produce millions of arbitrary-shaped nano-patterns in a parallel manner [50], but it could be further extended to obtain only single lines or patterns if a tight focus spot is employed to irradiate fewer or only one micro-sphere along its scanning path. The sub-micro/micro-structures obtained in this paper can be refined to attain specific dimensions in diameter, depth, shape, and periodicity so they can be used as anti-reflective surfaces for solar-cell applications or as photonic structures with a structural colour function to be employed as pixels in reflective colour displays [51]. More applications include the fabrication of single nano-channels and soft-marking of materials in which size of marks is crucial.

5 Conclusion

We have presented an extended application for a near-field laser nano-fabrication technique that combines conventional direct laser micro-processing and a particle-assisted laser nanofabrication technique to generate micro-patterns that are composed of sub-micrometre/micro-structures. This was demonstrated by rapid scanning a focused $Nd{:}YVO_4$ laser beam over a self-assembled particle lens array of SiO_2 micro-spheres on top of a Si surface, however more work is being undertaken in order to produce finer micro/nano-patterns. The obtained sub-micrometre patterns have the potential to replicate natural photonic crystals, such as the "moth eye" and "butterfly wing scale" structures.

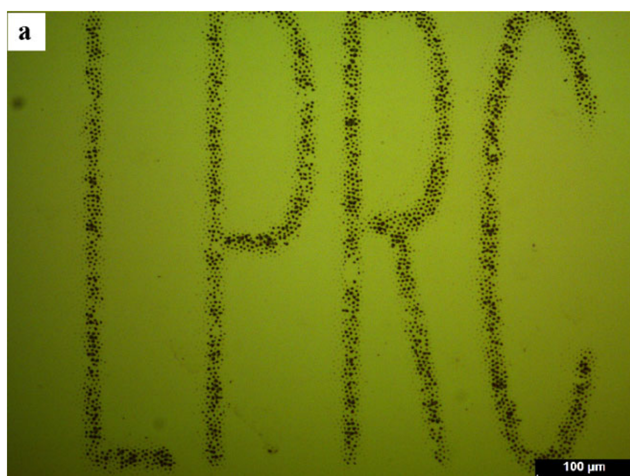

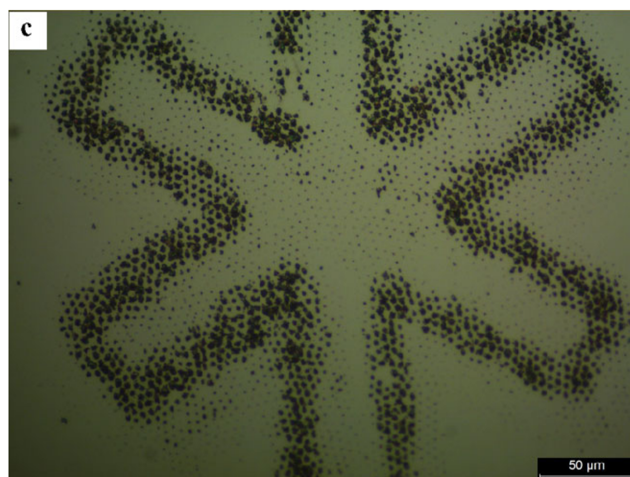

Fig. 7 (**a–b**) Laser-scribed patterns made of sub-micrometre structures when a focused laser beam was scanned over a 5 μm SiO_2 monolayer at a fluence of 170 mJ/cm^2. Patterns are visible due to the scattering effects of the sub-micro/micro-structures

Acknowledgements One of the authors (AP) gratefully acknowledges the full support from the Mexican Council for Science and Technology (CONACYT).

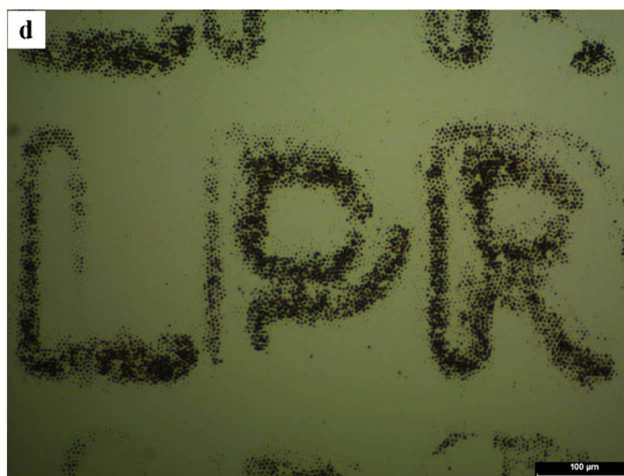

Fig. 7 (*Continued*)

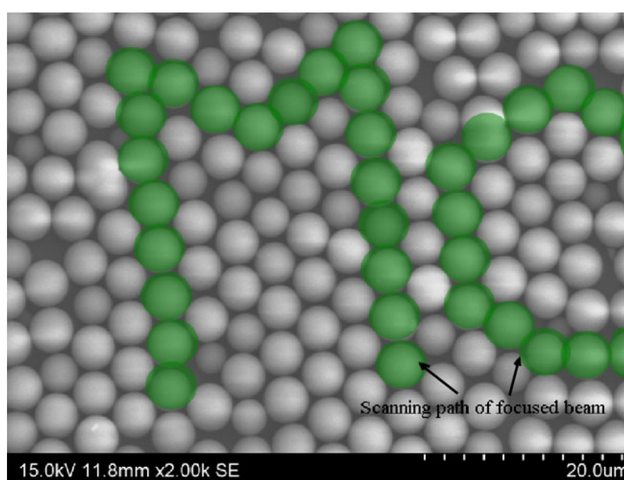

Fig. 8 SEM micrograph of a self-assembled monolayer of SiO_2 micro-spheres and the proposed scanning path of a focused beam in order to fabricate micro/nano-arbitrary patterns by employing the CPLA technique

References

1. C. Sanchez, H. Arribart, M.M.G. Guille, Nat. Mater. **4**, 277–288 (2005)
2. A. Parker, H. Townley, Nat. Nanotechnol. **2**, 347–53 (2007)
3. Z. Vértesy, Zs. Bálint, K. Kertész, J.P. Vigneron, V. Lousse, L.P. Biró, J. Microsc. **224**, 108–110 (2006)
4. P. Vukusic, Physicist **41**, 9–14 (2004)
5. P. Vukusic, Phys. Today **59**, 82–83 (2006)
6. P. Lalanne, G.M. Morris, Nanotechnology **8**, 53–56 (1997)
7. S.H. Zaidi, C. Matzke, L. Koltunski, K. DeZetter, in *Conference Record of the IEEE Photovoltaic Specialists Conference*, Lake Buena Vista, FL, US, 2005, pp. 1145–1148
8. S.J. Wilson, M.C. Hutley, Opt. Acta **29**, 993–1009 (1982)
9. M.E. Motamedi, W.H. Southwell, W.J. Gunning, Appl. Opt. **31**, 4371–4376 (1992)
10. K. Hadobas, S. Kirsch, A. Carl, M. Acet, E.F. Wassermann, Nanotechnology **11**, 161–164 (2000)
11. E.B. Grann, M.G. Moharam, D.A. Pommet, J. Opt. Soc. Am. A **12**, 333–339 (1995)

12. P. Vukusic, J.R. Sambles, C.R. Lawrence, Proc. R. Soc. Lond. B, Biol. Sci. **271**, 237–239 (2004)
13. Z. Yu, H. Gao, W. Wu, H. Ge, S.Y. Chou, J. Vac. Sci. Technol. B, Microelectron. Nanometer Struct. Process. Meas. Phenom. **21**, 2874–2877 (2003)
14. C.J.M. Van Rijn, J. Microlithogr. Microfabr. Microsyst. **5**, 011012 (2006)
15. C.-H. Sun, P. Jiang, B. Jiang, Appl. Phys. Lett. **92**, 061112 (2008)
16. H. Sai, Y. Kanamori, K. Arafune, Y. Ohshita, M. Yamaguchi, Prog. Photovolt. **15**, 415–423 (2007)
17. A. Ritucci, A. Reale, P. Zuppella, L. Reale, P. Tucceri, G. Tomassetti, P. Bettotti, L. Pavesi, J. Appl. Phys. **102**, 034313 (2007)
18. S. Kwon, W. Chang, S. Jeong, in *Proceedings of SPIE*, Nara, Japan, 2004, pp. 57–61
19. J.-H. Klein-Wiele, J. Bekesi, J. Ihlemann, P. Simon, in *Proceedings of SPIE*, St. Petersburg, Russian Federation, 2004, pp. 139–146
20. Y. Kanamori, K. Hane, H. Sai, H. Yugami, Appl. Phys. Lett. **78**, 142–143 (2001)
21. M. Halbwax, T. Sarnet, P. Delaporte, M. Sentis, H. Etienne, F. Torregrosa, V. Vervisch, I. Perichaud, S. Martinuzzi, Thin Solid Films **516**, 6791–6795 (2008)
22. A. Fisher, M. Kuemmel, M. Jarn, M. Linden, C. Boissiere, L. Nicole, C. Sanchez, D. Grosso, Small **2**, 569–574 (2006)
23. H.L. Chen, S.Y. Chuang, C.H. Lin, Y.H. Lin, Opt. Express **15**, 14793–14803 (2007)
24. H.L. Chen, K.T. Huang, C.H. Lin, W.Y. Wang, W. Fan, Microelectron. Eng. **84**, 750–754 (2007)
25. Z.B. Wang, M.H. Hong, B.S. Luk'yanchuk, Y. Lin, Q.F. Wang, T.C. Chong, J. Appl. Phys. **96**, 6845–6850 (2004)
26. E.W. Rothe, R.J. Baird, C.W. Manke, R. Piparia, Nanotechnology **19**, 165301 (2008)
27. R. Piparia, E.W. Rothe, R.J. Baird, Appl. Phys. Lett. **89**, 223113 (2006)
28. S.M. Huang, Z. Sun, Y.F. Lu, Nanotechnology **18**, 025302 (2007)
29. Z.B. Wang, W. Guo, A. Pena, D.J. Whitehead, B.S. Luk'yanchuk, L. Li, Z. Liu, Y. Zhou, M.H. Hong, Opt. Express **16**, 19706–19711 (2008)
30. D.R. Halfpenny, D.M. Kane, J. Appl. Phys. **86**, 6641–6646 (1999)
31. D.M. Kane, D.R. Halfpenny, J. Appl. Phys. **87**, 4548–4552 (2000)
32. Y. Kawata, C. Egami, O. Nakamura, O. Sugihara, N. Okamoto, M. Tsuchimori, O. Watanabe, Opt. Commun. **161**, 6–12 (1999)
33. B.S. Luk'yanchuk, Y.W. Zheng, Y.F. Lu, in *Proceedings of SPIE*, USA, 2000, pp. 576–587
34. M. Mosbacher, H.J. Munzer, J. Zimmermann, J. Solis, J. Boneberg, P. Leiderer, Appl. Phys. A **72**, 41–44 (2001)
35. H.J. Munzer, M. Mosbacher, M. Bertsch, J. Zimmermann, P. Leiderer, J. Boneberg, J. Microsc. **202**, 129–135 (2001)
36. K. Piglmayer, R. Denk, D. Bauerle, Appl. Phys. Lett. **80**, 4693–4695 (2002)
37. Y. Lu, S.C. Chen, Nanotechnology **14**, 505–508 (2003)
38. B.S. Luk'yanchuk, N. Arnold, S.M. Huang, Z.B. Wang, M.H. Hong, Appl. Phys. A **77**, 209–215 (2003)
39. Z.B. Wang, N. Joseph, L. Li, B.S. Luk'yanchuk, J. Mech. Eng. Sci. **224**, 1113–1127 (2009). doi:10.1243/09544062JMES176
40. C.M. Othon, A. Laracuente, H.D. Ladouceur, B.R. Ringeisen, Appl. Surf. Sci. **255**, 3407–3413 (2008)
41. M. Ulmeanu, M. Zamfirescu, L. Rusen, C. Luculescu, A. Moldovan, A. Stratan, R. Dabu, J. Appl. Phys. **106** (2009)
42. F. Hubenthal, R. Morarescu, L. Englert, L. Haag, T. Baumert, F. Trager, Appl. Phys. Lett. **95** (2009)
43. R. Tsu, R.T. Hodgson, T. Teh Yu, J.E. Baglin, Phys. Rev. Lett. **42**, 1356–1358 (1979)
44. A. Kiani, K. Venkatakrishnan, B. Tan, Opt. Express **17**, 16518–16526 (2009)
45. Y. Izawa, Y. Setuhara, M. Hashida, M. Fujita, Y. Izawa, Jpn. J. Appl. Phys. **45**, 5793–5794 (2006)
46. M. Pervolaraki, P.E. Dyer, P. Monk, Appl. Phys. A **79**(4–6), 849–854 (2004)
47. C. Tai-Chang, R.B. Darling, J. Mater. Process Technol. **169**, 214–218 (2005)
48. J.H. Yoo, S.H. Jeong, R. Greif, R.E. Russo, J. Appl. Phys. **88**, 1638–1649 (2000)
49. D. Bäuerle, *Laser Processing and Chemistry* (Springer, Heidelberg, 2000)
50. W. Guo, Z.B. Wang, L. Li, D.J. Whitehead, B.S. Luk'yanchuk, Z. Liu, Appl. Phys. Lett. **90**, 243101 (2007)
51. F. Micheron, Mol. Cryst. Liq. Cryst. **446**, 255–259 (2006)